Thermal, effective and exergetic analysis of double flow packed bed solar air heater

Saket Kumar[*], Abhishek Priyam, R.K. Prasad

Department of Mechanical Engineering, NIT Jamshedpur, Jharkhand, India

Corresponding Author Email: saket.gec@gmail.com

ABSTRACT

An experimental investigation has been performed to study the thermal, effective and exergetic performances of a double flow packed bed solar air heater having wire mesh as porous packing in its upper duct. The experiment is encompassed with the variables like packing bed height, mass flow rate of air and the solar radiation intensity. Experimental data has been collected for specified range of system and operating parameters to calculate the temperature rise parameter, thermal efficiency, effective efficiency, entropy generation and exergetic efficiency and to study the effects of system and operating parameters. Also, comparisons of packed bed solar air heater with that of smooth solar air heater of the conventional type have been presented. The results of experimental analysis on the performance of double flow packed bed solar air heater with wire mesh packing in the upper duct can be useful in designing such solar air heaters.

1. INTRODUCTION

Solar air heaters have been widely used because of their inherent simplicity and low manufacturing cost. The major application of solar energy collector is to heat the fluids. It is also used for drying of vegetables, fruits, grains and other agricultural products and in industries for various heating and cooling purposes. Exergy efficiency is generally used to introduce and compare thermal systems including flat plate solar collectors despite the fact that the first law of thermodynamics is not solely capable of demonstrating its quantitative and qualitative performances. The main part of flat plate collector is a single black absorber plate which absorbs solar energy and transfers the thermal energy to a carrier fluid (air or water). Because of this, the thermal efficiency of the collector is comparatively lower. Use of porous packing material in the collector duct considerably enhances the energy collection and heat transfer rates by increasing heat transfer coefficient between the carrier fluid and absorber in the solar collector duct. Akpinar and kocyigit [1] made an experimental analysis of a new flat plate solar air heater with various obstacles and without obstacles. In this work first and second law efficiencies were determined for solar air heaters and also compared them. Leiner et al. [2] optimized the design of absorber and flow duct by maximizing the net energy flow. Bahrehmand et al. [3] studied the energy and exergy analysis of different solar air heaters with forced convection. In this work, a mathematical model was developed for simulating the thermal behavior of single and two glass covers solar air heating systems with forced convection flow and concluded that the systems with fin are more efficient than other existing systems from the energy and exergy efficiencies point of view. Benli [4] carried out experimental analysis to determine energy and exergy efficiency of a new solar air heater having different surface shapes with an aim to provide a remedy for the low thermophysical properties of air which is used at different

absorber surface of air heater. This work focused on the experimental performance of four types of air heating solar collectors: reverse corrugated, base flat-plate corrugated, trapeze and reverse trapeze for exergy analysis. Bouadila et al. [5] carried out energy and exergy analysis of a new solar air heater having a packed bed latent heat energy storage system using Phase Change Material in the form of spherical capsules and optimized the energy and exergy efficiency based on first and second laws of thermodynamics respectively for obtaining the performance of the system on the basis of temperature distribution in different parts of the collectors. Chen et al. [6] investigated experimentally the comparative study of different flat plate solar collectors and the traditional metal solar collectors and solar collectors specimens fabricated from polymeric materials and concluded that the efficiency of a polymeric collector is 8-15 % lower than the efficiency of a traditional collector. Esen [7] presented experimentally the energy and exergy analysis of double flow solar air heater having different obstacles on absorber plates. Farzaneh-Gord et al. [8] proposed a new system, which is having the feasibility of employing solar heat storage system in terms of fuel provided and energy destruction rate. Fudholi et al. [9] reviewed the solar drying system with air based solar collectors, which are environmentally friendly. Golneshan and Nemati [10] did the analysis of energy of unglazed transpired solar collectors (UTG). They found the optimum working temperature and suggested to determine the most effective and least expensive geometry. Panwar et al. [11] reviewed on energy and exergy analysis of solar drying systems and analyzed a holistic approach on energy and exergy of a solar dryer. Park et al. [12] Studied the energy and exergy analysis of typical renewable energy systems. Sabzpooshani et al. [13] evaluated theoretically the exergetic performance of a single pass baffled solar air heater and investigated the effect of variation of fin and baffle parameters, the number of glass covers, bottom insulation thickness and inlet air temperature at

different mass flow rates on the exergy efficiency. Soundararajan et al. [14] established the energy flow diagrams in the form of Sankey diagrams as a useful tool in energy managements and performance improvement. Ucar and Inalli [15] investigated experimentally the thermal and exergy analysis of solar air collectors with passive augmentation technique and concluded that the largest irreversibility is occurring at the conventional solar collector in which collector efficiency is smallest. Yadav et al. [16] evaluated the exergetic efficiency of roughened solar air heater duct provided with protrusions arranged in arc fashion over the absorber plate. Singh et al. [17] analytically investigated the thermal performance characteristics of artificially roughened double flow solar air heater and reported that the performance can be enhanced by using roughness on both sides of the absorber plate. Kurtbas and Durmus [18] performed the efficiency and exergy analysis of a new solar air heater by considering fire solar collectors with four different cases and evaluated the heat transfer and pressure loss depending on shape and number of absorbers. Nwosu [19] optimized the exergy analysis on pin fins in the design of an absorber in a solar air heater which improves the heat absorption and dissipation potential of a solar air heater. Lalji et al. [20] evaluated the exergy analysis of packed bed solar air heater and also investigated experimentally the heat transfer and friction factor for flow in a packed bed solar air heater at different mass flow rates of air for various porosities and shape of matrices. Jafarkazemi and Ahmadifard [21] studied the effect of parameters on the energy and exergy efficiency of flat plate collector. Oztop [22] reviewed the energetic and exergetic aspects of solar air collectors varied from 47% and 89%. Bayrak et al. [23] studied the performance assessment of porous baffles inserted solar air heaters using energy and exergy analysis method and obtained that the highest collector efficiency and air temperature rise are achieved by solar air heater with baffle thickness of 6 mm and air mass flow rate of 0.025 kg/s. Kalogirou et al. [24] reported the exergy analysis on solar thermal systems. Sahu and Prasad [25] made an investigation on exergetic performance evaluation of solar air heater with arc-shaped wire rib roughened absorber plates. They studied the effect of roughness parameters on exergy efficiency. Sharma et al. [26] investigated experimentally the thermal performance of a single flow solar air heater having its duct packed with blackened wire screen matrices. They concluded that thermal performance of plane collector is improved appreciably by packing its duct with blackened wire-screen matrices and this improvement is a strong function of the bed and operating parameters. Yeh et al. [27] investigated experimentally the collector efficiency of double flow solar air heaters with fins attached over and under the absorber plate. Karim & Hawlader [28] investigated performance of flat plate, v-corrugated and finned air collectors for a wide range of operating and design conditions.

A review of the above literature indicates that no experimental investigation on the performance analysis of the double flow SAH, having its upper duct packed with porous absorber in the form of blackened wire screens and lower duct as smooth, has been reported. In view of this, the present study aims to investigate experimentally the thermal, thermohydraulic and exergetic efficiencies of a double flow packed bed SAH. The effects of system and operating parameters on the performance of double flow packed bed SAH have also been studied.

2. DESCRIPTION OF EXPERIMENTAL WORK

2.1 Experimental set-up

The experimental set up, consisting of a single flow smooth plate SAH and a double flow SAH, has been designed and fabricated for the experimentation. Blackened wire screens have been used as the porous packing material only in the upper duct of double flow solar air heater as shown in Fig.1. The Pictorial view of the experimental set-up has been shown in Fig.2.The main components of the experimental set up are, wooden rectangular double ducts comprising flow straightener and test section, G.I pipes, blower, control valve, orifice meter, U-tube manometer, and thermocouples etc. The total length of the rectangular duct is 3250 mm in which the flow straightener is of 1000 mm and the test section is of 2250 mm length respectively as shown in Fig.1. The internal dimensions of both the lower and upper ducts are 2250 mm × 400 mm × 30 mm. The indoor experiment was conducted by using a halogen lamp (0-1500 W/m²) as the source of radiation energy. The intensity of the lamp was varied from 750- 1050 W/m² with the help of a regulator as per requirement of the experiment. Orifice meters have been used to measure the mass flow rates of air in the ducts, as well as the total mass flow rate of air flowing through the duct. The calibration of the orifice meter was done with the help of a calibrated orifice plate. Glass wool was used as insulating material at bottom of the test section to minimize heat losses to the surrounding. The temperature of the air at various positions of the test sections were measured by using calibrated J-type thermocouples. These thermocouples were connected to a data logger for digital display. The various positions of the thermocouples to measure air temperature are shown in Fig.3. The side view of double flow packed bed solar air heater test section has been shown in Fig.4.

2.2 Experimentation

Experiments were conducted on the set up consisting of double flow solar air heater ducts with blackened wire mesh packing in its upper duct and smooth absorber plate solar air heater in order to collect the data for analysis. A view of wire mesh is shown in Fig.5.After inspection of correct functioning of all the instruments and the leak-proof of the joints, the blower was switched on. Five values of mass flow rates in the range of 0.016-0.036 kg/s were considered for each height of wire mesh packing. The mass flow rate of air was varied with the help of control valves. The mass flow rate in upper duct was fixed as 0.25M and in the lower duct, it was fixed at 0.75M, M is the total mass flow rate of air. After fixing the total mass flow rate at different fractions, the various values were recorded when the system approached quasi-steady state. In this study, the effect of packing height on the upper duct has been examined on the air temperature rise parameter and thermal efficiency. Also, the effect of an operating parameter such as mass flow rate has also been examined. For a given height of wire screens, the mass flow rate has been varied and outlet temperatures have been measured by thermocouples.
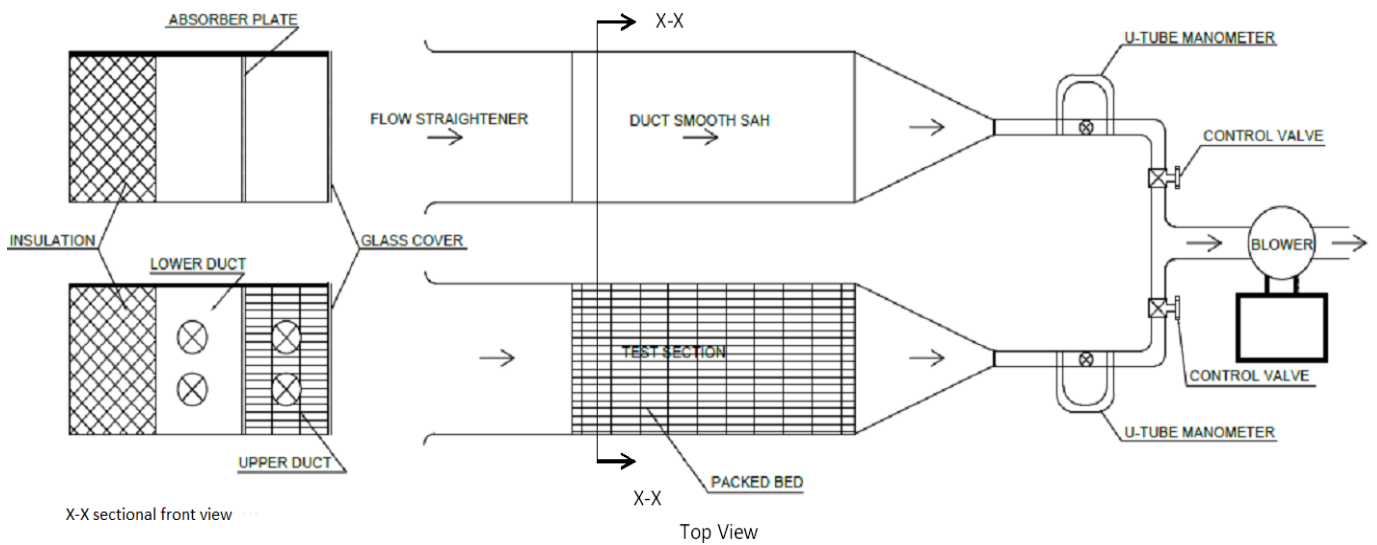
Figure 1. Schematic diagram of Experimental set up of a double flow packed bed solar air heater
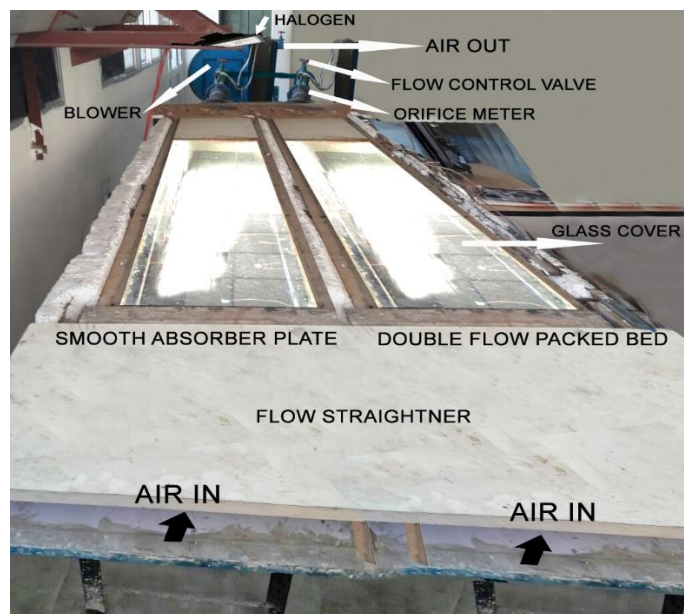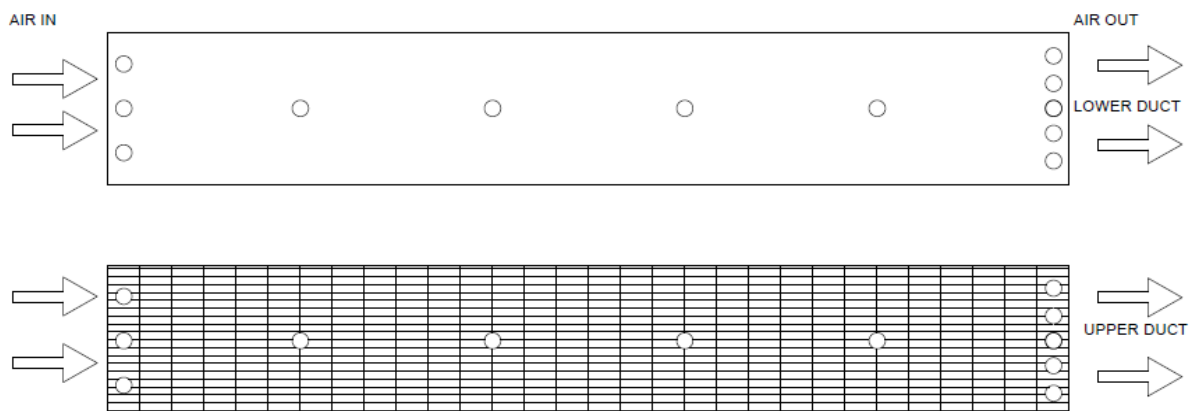

Figure 2. Pictorial view of Experimental set-up

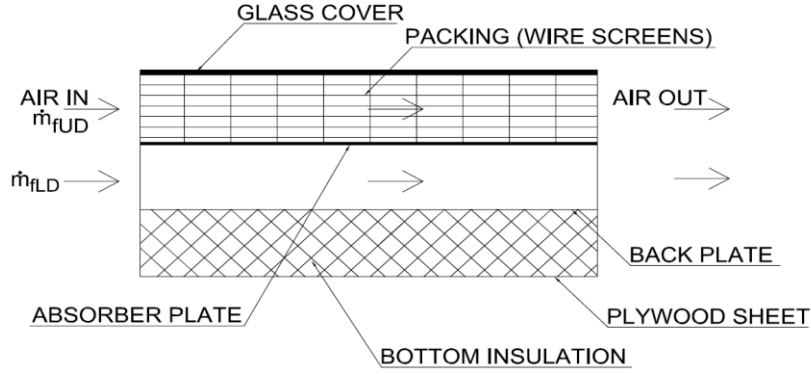**Figure 3.** Positions of thermocouples to measure the air temperature in the test sections.

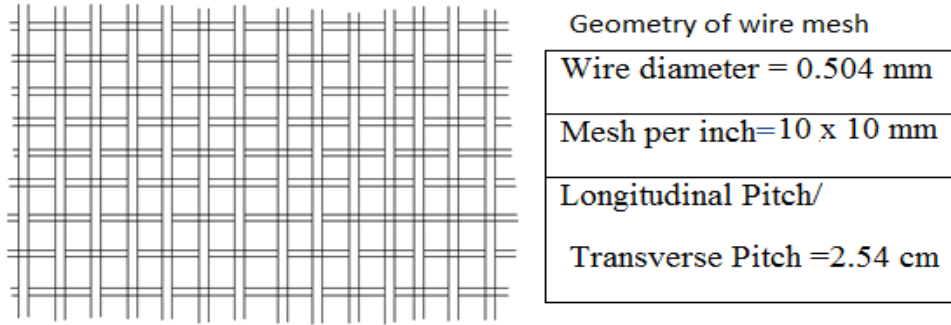**Figure 4.** Side view of double–flow packed bed solar air heater test section

Figure 5. A view of wire mesh screen

2.3 Data reduction

(A) Thermal and thermohydraulic (effective) performances

The collected data were used to calculate the rise in temperature of the air and thermal efficiency of double flow packed bed solar air heater with blackened wire screen packing in the upper duct. The equations used to calculate thermal efficiency are given below.

$$\dot{m}_{UD} = C_d A_o \sqrt{\frac{2\rho \Delta P_{UD}}{1-\beta^4}} \tag{1}$$

$$\Delta P_{UD} = 9.81\rho(\Delta h_o)_{UD} \tag{2}$$

$$\dot{m}_{LD} = C_d A_o \sqrt{\frac{2\rho \Delta P_{LD}}{1-\beta^4}} \tag{3}$$

$$\Delta P_{LD} = 9.81\rho\left(\Delta h_o\right)_{LD} \tag{4}$$

$$M = \dot{m}_{UD} + \dot{m}_{LD} \tag{5}$$

The useful energy gain by air in upper channel and lower channel are respectively,

$$Q_{UD} = MRC_P \left(T_{fo_{UD}} - T_{fi_{UD}}\right) \tag{6}$$

and,

$$Q_{LD} = M\left(1-R\right)C_P \left(T_{fo_{LD}} - T_{fi_{LD}}\right) \tag{7}$$

$$\eta_{th} = \frac{MC_P \left(T_0 - T_i\right)}{IA_c} \tag{8}$$

$$T_o = \frac{T_{foUD} + T_{foLD}}{2} \tag{9}$$

$$T_i = \frac{T_{fiUD} + T_{fiLD}}{2} \tag{10}$$

In calculations, the thermophysical properties of air were used corresponding to bulk mean temperature of air.

The Mechanical Power (P_m), required to overcome the resistance against flow of air in the duct was determined using measured value of pressure drop (ΔP_d) along the duct,

$$(P_m)_{UD} = \frac{\dot{m}_{UD}\Delta P_{UD}}{\rho} \text{ and } (P_m)_{LD} = \frac{\dot{m}_{LD}\Delta P_{LD}}{\rho} \tag{11}$$

where the subscripts *UD* and *LD* stand for upper duct and lower duct respectively.

The net energy gain, Q_{net} of the collector was calculated using the equation,

$$Q_{net} = Q_u - \frac{P_m}{C} \tag{12}$$

where,

$$Q_u = Q_{UD} + Q_{LD}$$
$$P_m = (P_m)_{UD} + (P_m)_{LD} \tag{13}$$

And C is the conversion factor that allows conversion of mechanical energy to equivalent thermal energy and is given by

$$C = \eta_{Th}\eta_{tr}\eta_m\eta_f \tag{14}$$

By considering the value of η_{Th} as 0.35, η_{tr} as 0.92, η_m as 0.88 and η_f as 0.65, the value of "C" is obtained as 0.184 [29].

The thermohydraulic or effective efficiency is calculated using the equation,

$$\eta_{effective} = \frac{Q_{net}}{IA_c} \tag{15}$$

(B) Exergetic performance

This article focuses on the use of the concept of exergy analysis which is based on the combined first and second laws of thermodynamics.

The assumptions made in the analysis are:

1. Steady state condition prevails.

2. Negligible effect of potential and kinetic energies and no chemical reaction.

3. Air is an ideal gas with a constant specific heat, and it is almost dry.

4. The directions of heat transfer to the system and work transfer from the system are positive.

The mass balance equation can be expressed in the rate form as.

$$\sum \dot{m}_{in} = \sum \dot{m}_{out} \tag{16}$$

where $\dot{m}$ is the mass flow rate, and the subscripts 'in' stands for inlet and 'out' for outlet.

When the effects due to the kinetic and potential energy changes are neglected, the general exergy balances can be expressed as given below [15],

$$\sum \dot{Ex}_{in} - \sum \dot{Ex}_{out} = \sum Ex_{dest} \tag{17a}$$

or

$$\dot{Ex}_{heat} - \dot{Ex}_{work} + \dot{Ex}_{mass,in} - \dot{Ex}_{mass,out} = \dot{Ex}_{dest} \tag{17b}$$

Eq. (17b), which represents the general exergy balance equation, can be expressed as follows:

$$\sum \left(1 - \frac{T_e}{T_s}\right)\dot{Q}_S - \dot{W} + \sum \dot{m}_{in}\psi_{in} - \sum \dot{m}_{out}\psi_{out} = \dot{Ex}_{dest} \tag{18}$$

where

$$\psi_{in} = (h_{in} - h_e) - T_e(s_{in} - s_e) \tag{19a}$$

$$\psi_{out} = (h_{out} - h_e) - T_e(s_{out} - s_e) \tag{19b}$$

$$\dot{W} = \frac{\dot{m}\Delta p}{\rho} \tag{20}$$

Substituting Eqs (19a), and (19b) in Eq (18), and then arranging an equation, as given below is obtained:

$$\left(1 - \frac{T_e}{T_s}\right)\dot{Q}_s - \frac{\dot{m}\Delta P}{\rho} - \dot{m}(h_{out} - h_{in}) - T_e(s_{out} - s_{in}) = \dot{Ex}_{dest} \tag{21}$$

where $\dot{Q}_s$ is the radiation energy absorbed by the collector absorber surface which is evaluated using the expression given below (Torres Reyes et al., 2003)

$$\dot{Q}_s = I(\tau\alpha)A_c \tag{22}$$

The change in the enthalpy and entropy of the air in the collector are expressed respectively by Ucar and, Inallı [15],

$$\Delta h = h_{out} - h_{in} = C_p(T_{f,out} - T_{f,in}) \tag{23}$$

$$\Delta s = s_{out} - s_{in} = C_p In \frac{T_{f,out}}{T_{f,in}} - RIn \frac{P_{out}}{P_{in}} \tag{24}$$

By substituting Eqs (22)-(24) into (21) the equation as given below can be derived

$$\left(1 - \frac{T_e}{T_s}\right)I(\tau\alpha)A_c - \frac{\dot{m}\Delta P}{\rho} - \dot{m}C_p\left(T_{F,out} - T_{f,in}\right)$$
$$+\dot{m}C_pT_e In \frac{T_{f,out}}{T_{f,in}} - \dot{m}RT_e In \frac{P_{out}}{P_{in}} = \dot{Ex}_{dest} \tag{25}$$

The exergy destruction or the irreversibility may be expressed as given below

$$\dot{Ex}_{dest} = T_e\dot{S}_{gen} \ , \ \Rightarrow \dot{S}_{gen} = \frac{\dot{Ex}_{dest}}{T_e} \tag{26}$$

The exergy efficiency of a solar air heating system can be evaluated by calculating the net output exergy of the system or exergy destruction in the system. Here the exergy efficiency of SAH system has been evaluated by considering net output exergy of the system. The second law efficiency is calculated as given below:

$$\eta_{II} = \frac{\dot{Ex}_{out}}{\dot{Ex}_{in}} = \frac{\dot{m}\left[h_{out} - h_{in} - T_e\left(s_{out} - s_{in}\right)\right]}{\left(1 - \frac{T_e}{T_s}\right)\dot{Q}_s} \tag{27}$$

2.4 Uncertainty analysis

There are always possibilities of some errors in experimental measurements, in spite of the care taken during experimentation. Therefore, it is necessary to determine the maximum possible error in experimental measurements. The

error analysis was carried out by estimating uncertainty in the experimental results, based on the raw data recorded by using the method suggested by Kline and McClintock [30]. If the value of any parameter is calculated using certain measured quantities then the error in the measurement of ''y'' (a parameter) is given as follow

$$\frac{\delta y}{y} = \left[\left(\frac{\partial y}{\partial x_1} \delta x_1 \right)^2 + \left(\frac{\partial y}{\partial x_2} \delta x_2 \right)^2 + \left(\frac{\partial y}{\partial x_3} \delta x_3 \right)^2 + ... + \left(\frac{\partial y}{\partial x_n} \delta x_n \right)^2 \right]^{0.5} \quad (28)$$

where $\delta x_1, \delta x_2, \delta x_3 .... \delta x_n$ are possible errors in the measurements of variables x_1, x_2, x_3, . . . x_n. δy is known as absolute uncertainty and .. is known as relative uncertainty. In the present investigation, the most important parameter is the thermal efficiency which depends on other parameters, has been considered for the uncertainty analysis as given in Appendix- 1.

In addition to this, the uncertainty analysis for some other parameters like Reynolds number and friction factor has also been made and shown Appendix- 1.

Calculated Uncertainty values:

S.No	Parameters	Uncertainty value	S.No	Parameters	Uncertainty value
1.	A_P	$\pm$ 0.0004617	5.	R_e	$\pm$ 0.0225
2.	A_o	$\pm$ 0.00208	6.	Q_u	$\pm$ 0.0272
3.	$\dot{m}$	$\pm$ 0.0198	7.	η_{th}	$\pm$ 0.02938
4.	V	$\pm$ 0.0208	8.	f	$\pm$ 0.0424

3. RESULTS AND DISCUSSION

The thermal efficiency, effective efficiency and the second law efficiency (exergetic efficiency) of the double flow solar air heater having upper duct packed with wire mesh and the lower duct as unpacked and that of conventional collector have been calculated using the experimental data collected for various mass flow rates and the system parameters and are discussed below.

Results have been compared with that of a single flow smooth absorber plate solar air heater to assess the enhancement in thermal efficiency, air temperature rise, effective efficiency and second law efficiency of the system, operating under similar experimental conditions.

Fig.6 represents the variation of thermal efficiency for the fraction R of total mass flow rate and different mass flow rate. Thermal efficiency increases with the increase in total mass flow rate. For a given mass flow rate, thermal efficiency decreases with the increase in the fraction of mass flow rate R. It can be seen from Fig.6. that the maximum thermal efficiency has been achieved at the minimum fraction of total mass flow rate.
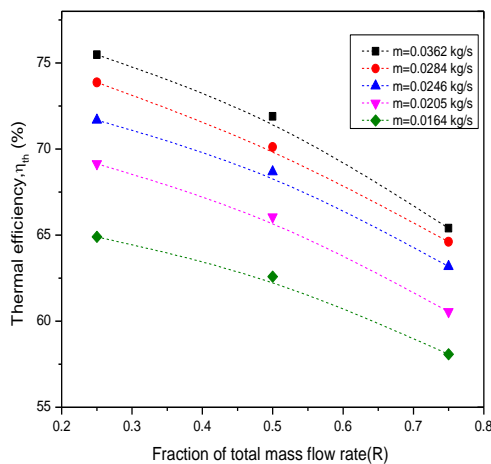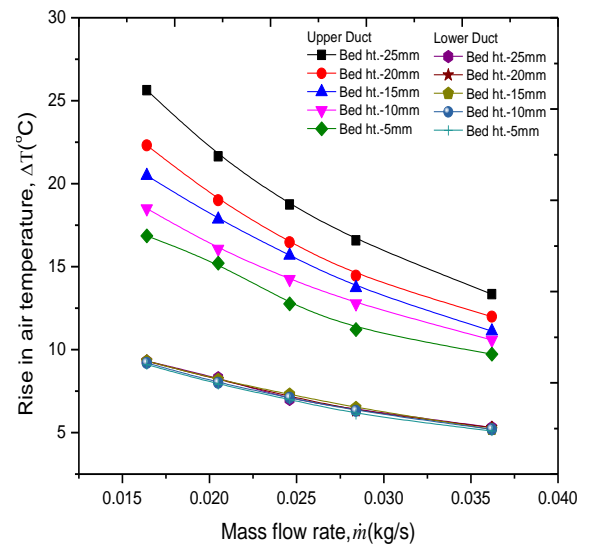

Figure 7. Rise in air temperature for the upper duct and lower duct

Figure 6. Thermal efficiency as a function of the fraction of total Mass flow rate for various mass flow rates
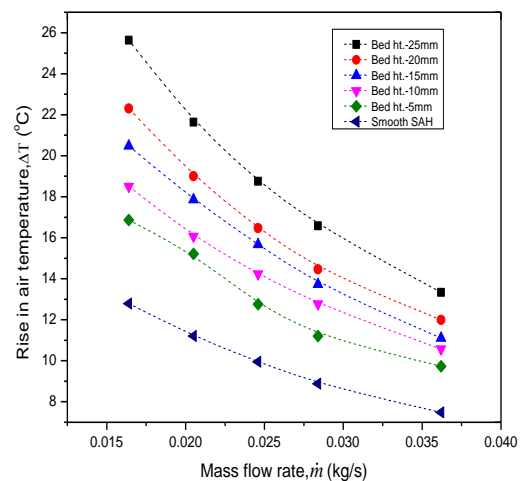

Figure 8. Variation of rise in air temperature with mass flow rate of air for different wire mesh bed height

The variation of Rise in air temperature in the upper duct and in the lower duct of double flow packed bed solar air heater with a mass flow rate of air has been shown in Fig.7. The maximum temperature rise has been obtained in the upper duct with a bed height of 25 mm, while for the lower duct the temperature rise is almost constant. These happen due to high transfer coefficient between the air heat transferring surface in the upper duct and due to low heat transfer rate coefficient in the lower duct.

Fig.8. shows the variation of rise in temperature with a mass flow rate of air at different bed heights of double flow packed bed solar air heater. It is observed that for a given bed height, the rise in air temperature decreases with the increase in mass flow rate. The smooth solar air heater also shows the same trend. This is because at the higher mass flow rate the air velocity becomes high and unable to pick up heat within the short duration. Also, the rise in air temperature increases with the increase in bed height for a given mass flow rate of air. This occurs due to the fact that the value of the thermal capacity $(\alpha\gamma c_P)$ of the packing material and the surface conductance $(\bar{h}A)$ increases with the increase in bed height and results in higher temperature rise. The maximum temperature rise of $25.8\,^{\circ}C$ has been achieved at the lower mass flow rate of 0.016 kg/s corresponding to the height of bed equal to 25 mm.
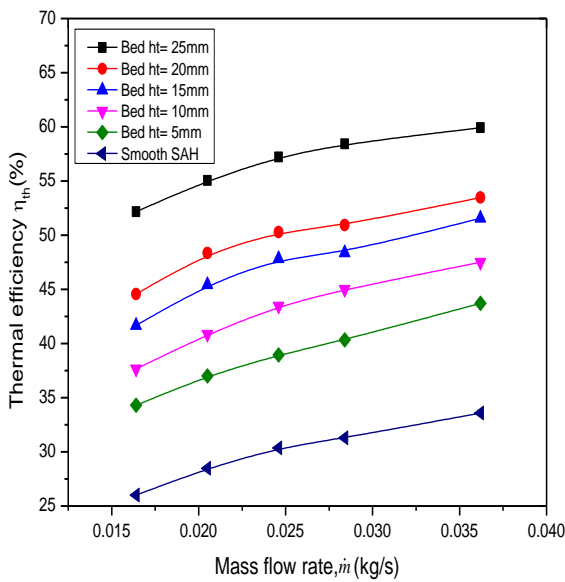

Figure 9. Variation of thermal efficiency with mass flow rate at different wire mesh bed height

Fig.9. shows the plot of thermal efficiency as a function of mass flow rate of air at different bed heights. The plots show that the thermal efficiency of SAH increases with the increase in mass flow rate for all values of bed heights considered. This occurs due to the fact that the increase in heat conductance $(\bar{h}A)$, the bed height of 25 mm maintains the enhanced efficiency for all the mass flow rates. An enhancement of 2.3 times has been achieved by double flow packed bed SAH for a packing height of 25 mm at a lower mass flow rate of 0.016 kg/s and 1.8 times at higher mass flow rate of 0.036 kg/s with respect to the smooth plate solar air heater.
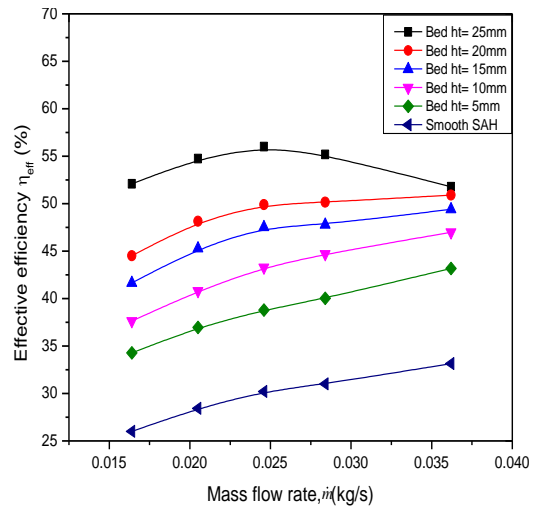

Figure 10. Variation of effective efficiency with mass flow rate at different wire mesh bed height

The evaluation of Effective efficiency includes both the evaluation of thermal energy gain by the flowing air and the pumping power needed to propel the air in the duct of SAH. Fig.10 shows the variation of effective efficiency with a mass flow rate of air at different bed heights. It is observed that the Effective efficiency increases with the increase in mass flow rate, attains the maximum value and then starts decreasing with further increase in mass flow rate at the bed height above 20 mm. At the highest bed height of 25 mm, the effective efficiency is the highest corresponding to the mass flow rate of air of 0.025 kg/s. The maximum enhancement in effective efficiency has been found in order of 1.98 times, 1.85 times and 1.54 times has been achieved at the mass flow rate of 0.016, 0.025 and 0.in036 kg/s respectively. The enhancement in effective efficiency reduces with mass flow rates because, after maxima, the effect of friction loss is dominating over the effect of heat conductance $(\bar{h}A)$, resulting in higher pressure drop and the decrease in effective efficiency.
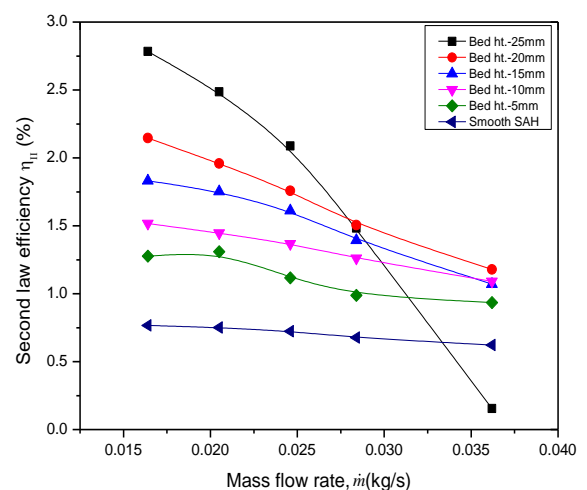

Figure 11. Variation of second law efficiency with mass flow rate at different wire mesh bed height

Fig.11. shows the variation of second law efficiency or exergetic efficiency with mass flow rate at different bed heights of the double flow packed SAH and for the smooth

collector. The second law efficiency decreases with increase in mass flow rate for all bed heights. However, after the mass flow rate of about 0.025 kg/s the bed height of 25 mm shows a drastic fall in second law efficiency because the effect of friction loss is dominating over the effect of heat transfer rate. Before the mass flow rate of 0.025 kg/s, the effect of heat transfer suppresses the power absorbed in overcoming the friction losses. For the lowest mass flow rate of 0.016 kg/s, second law efficiency reaches a maximum efficiency of 2.78
% for absorber bed height of 25 mm. The second law efficiency of smooth absorber plate SAH also decreases with a mass flow rate of air but with a very slow rate.
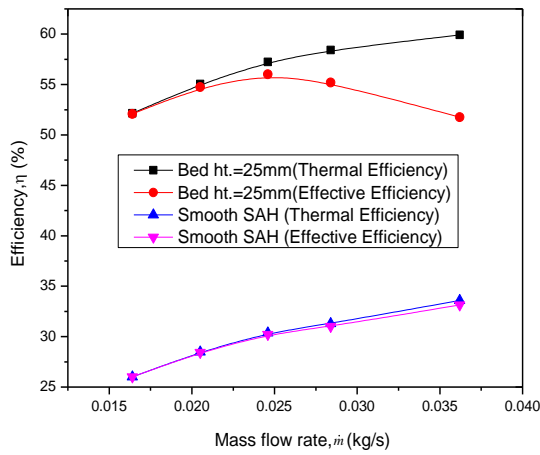

Figure 12. Variation of Thermal Efficiency and Effective efficiency with Mass flow rate at bed height=25mm

Fig.12. shows the variation of thermal efficiency and effective efficiency with mass flow rate for packed bed collector at a bed height of 25 mm and the smooth collector. It is clearly seen from the plot that the thermal efficiency of packed solar air heater increases with the increases in mass flow rate but the effective efficiency first increases and then decreases with the increase in mass flow rate. This is because up to a maximum gain of thermal energy the effect of friction loss is suppressed by the rate of heat transfer beyond that the power expended in overcoming the friction increases. The thermal and effective efficiencies, both increase with mass flow rate, as shown in Fig 12 for the smooth plate SAH.
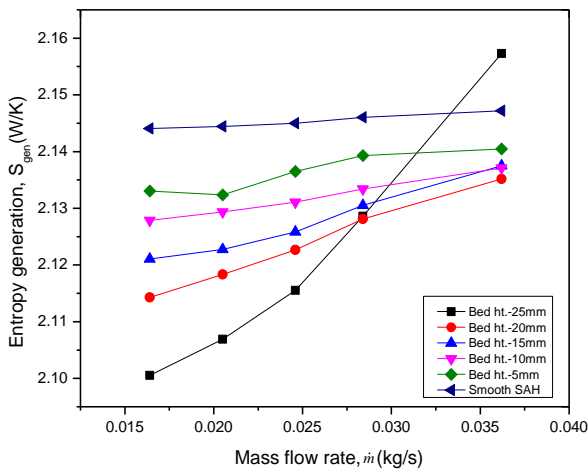

Figure 13. Variation of Entropy generation with Mass flow rate at different wire mesh bed heights.

Fig.13. shows the variation of entropy generation with a mass flow rate of air at different bed heights of the packed bed collector. It is seen from the plot that the entropy generation increases with increase in mass flow rate for all of the bed heights of the packed bed collector. The entropy generation rate of the SAH increases with the decrease in height of the packed bed at a given mass flow rate of air, however, it increases drastically at a higher mass flow rate (beyond 0.025 kg/s) for the bed height=25 mm. At this bed height, the pressure drop along the packed bed collector increases. This is because the higher mass flow rate leads to a lower rate of heat transfer as compared to increase in friction power losses. The entropy generation rate is the highest and also has the least variation with a mass flow rate of air in case of smooth plate SAH.
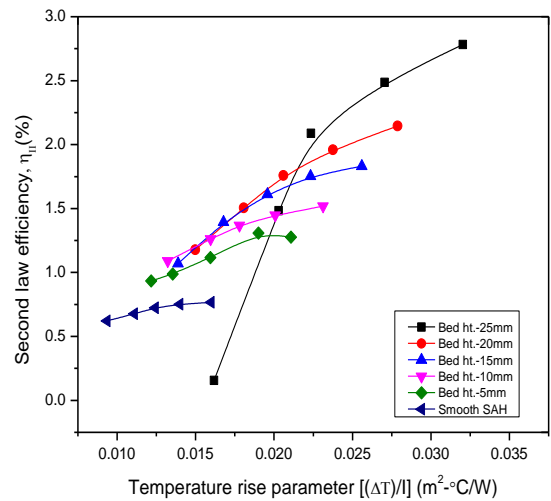

Figure 14. Variation of Second law efficiency with $\Delta T/I$ at different wire mesh bed heights.

Fig.14. shows the variation of second law efficiency with temperature rise parameter $\Delta T/I$ at different bed heights of packed bed and smooth SAH, which is also the performance plot based on second law efficiency. It can be seen from the plot that the higher value of $\Delta T/I$ leads to higher second law efficiency for a given height of packed bed. Heat conductance is the product of average heat transfer coefficient and heat transfer area. Enhancement in $\left(\bar{h}A\right)$, heat conductance enhance the heat transfer rate. For the lower, the effect of friction dominates the overall heat conductance $\left(\bar{h}A\right)$. The highest second law efficiency has been achieved for the bed height of 25 mm. It is observed that for the bed height of 25 mm the exergetic efficiency of the packed bed SAH increases sharply in the range of $\Delta T/I$ between 0.015-0.0225 $m^2 - {}^\circ C/W$ and beyond $\Delta T/I = 0.0225$ $m^2 - {}^\circ C/W$ it increases with a slower rate.
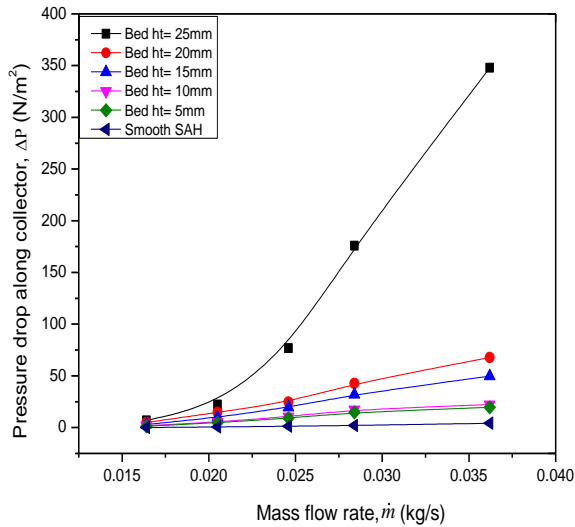
Figure 15. Variation of pressure drop along the collector with mass flow rate at different wire mesh bed heights

Fig.15 shows the variation of pressure drop along the collector with mass flow rate at different bed heights. For all the bed height from 5mm to 25mm, pressure drop increases with the increases in mass flow rate from 0.0164 kg/s to 0.0362 kg/s. Maximum pressure drop of 354 N/m^2 has been found for the maximum bed height of 25 mm at higher mass flow rate of 0.0362 kg/s. This is because up to minima, the effect of overall conductance $\left(\overline{h}A\right)$ and thermal capacity $\left(\alpha\gamma c_p\right)$ are dominating as compared to friction loss. After minima, the effect of friction loss is dominating over the thermal capacity and the overall conductance.
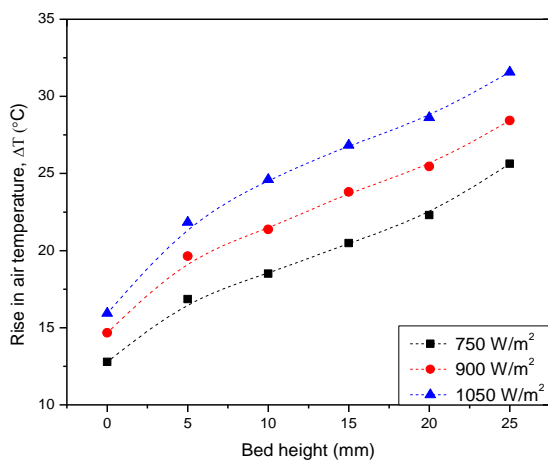

Figure 16. Variation of rise in air temperature with bed height for different heat flux

Fig.16 shows the rise in air temperature ΔT as a function of bed height for various values of radiation intensity. The higher value of radiation intensity leads to higher value of rise in air temperature. This is because at higher value of radiation intensity more heat is absorbed by the absorber and also transferred to the air passing through it.
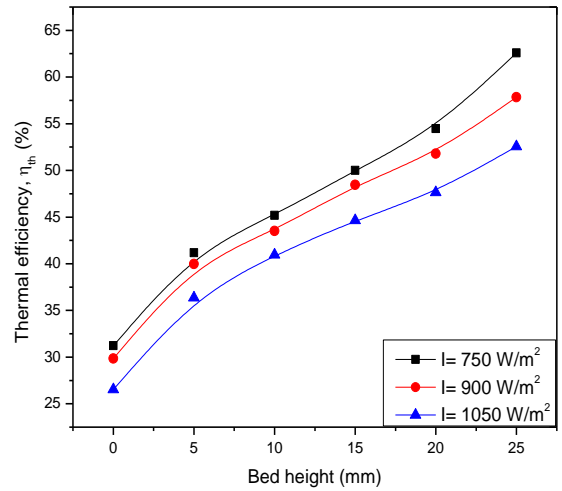

Figure 17. Thermal efficiency as a function of bed height for various heat flux

Fig.17 shows the variation of thermal efficiency with bed height for different intensity of radiation. As is obvious, the thermal efficiency increases with the increase in bed height for a given value of intensity of radiation. Also the thermal efficiency of air heater is the highest at the highest value of radiation intensity corresponding to a given bed depth.

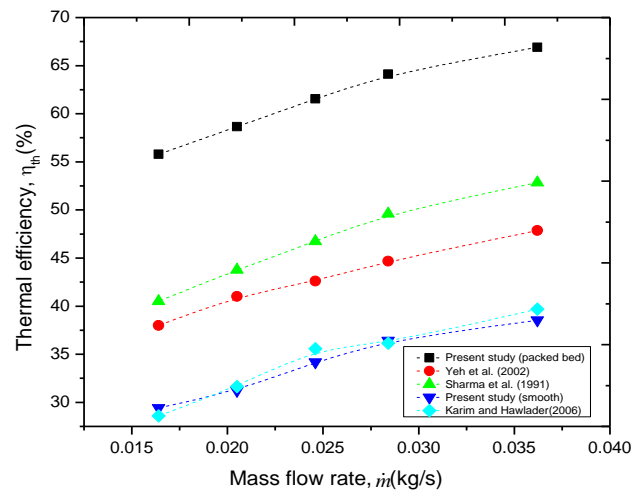## 4. VALIDATION OF EXPERIMENTAL ANALYSIS

Figure 18. Comparison of thermal efficiency obtained in present study with those available in literature

Fig.18. shows the comparison of thermal efficiency of double flow packed bed solar air heater (present work) and single flow smooth solar air heater with those of the double flow solar air heater having finned absorber plate [27], packed bed solar air heater [26] and single flow smooth absorber plate solar air heater [28] for specific values of bed height and intensity of radiation, an average deviation of ± 3.57% in thermal efficiency for the smooth solar air heater (present work) and that of the [28] has been found. A maximum enhancement of 37.5% and 46.7% in thermal efficiency for double flow with finned absorber plate [28] and that of the single flow with wire screens packed bed solar air heaters respectively has been found at the total mass flow

rate of 0.0164 kg/s. This shows that the use of double flow packed bed solar air heater having wire screens as a porous absorber in upper duct has better performance than double flow solar air heater, with finned absorber plate and that of single flow wire screen packed bed solar air heater. Also in comparison to smooth solar air heater, an enhancement of 2.11 times in thermal efficiency at lowest mass flow rate has been noticed. The variation of thermal efficiency with mass flow rate for the present investigation follows the same trend as those of other SAH$_s$, [26-28], which validates the results of the present investigation.

5. CONCLUSION

On the basis of experimental analysis of the double flow, solar air heater having the wire mesh packing in the upper duct and lower duct unpacked and a single flow smooth absorber plate SAH$_s$, the following conclusions can be drawn:

1. An enhancement in the thermal efficiency and temperature rise parameter of double flow collector having its upper duct packed with wire mesh absorber can be obtained up to 1.51 and 2.03 times respectively corresponding to a given height of packing and mass flow rate of air in the duct.

2. Thermal efficiency, effective efficiency and second law efficiency (exergetic efficiency) strongly depends on the wire mesh packed bed height of a double flow packed bed SAH. The maximum value of thermal efficiency, effective efficiency, and exergetic efficiency are found as 60.11%, 54.8% and 2.75% at the bed height of 25 mm respectively.

3. The increase in mass flow rate of air through the collector duct not only increases the thermal efficiency but also increases the pressure drop and thus reduces the effective efficiency.

4. The entropy generation rate of the double flow packed bed SAH decreases with the increase in bed height for a given mass flow rate of air. It has the lowest value for a bed height of 25 mm corresponding to mass flow rate of 0.016 kg/s but it increases drastically beyond the mass flow rate of 0.025 kg/s.

5. The double flow air heating collector with wire mesh packing in upper duct has higher thermal efficiency than the double flow finned absorber and also than the single flow wire screen packed bed solar air heater as well as single flow smooth absorber plate solar air heater.

REFERENCES

[1] Kavak AE, Fatih K (2010). Energy and exergy analysis of a new flat-plate solar air heater having different obstacles on absorber plates. Applied Energy 87: 3438-3450. https://doi.org/10.1016/j.apenergy.2010.05.017.

[2] Altfeld K, Leiner W, Fiebig M (1988). Second law optimization of flat-plate solar air heaters. Solar Energy 2: 127-132.

[3] Bahrehmand D, Ameri M, Gholampour M. (2015). Energy and exergy analysis of different solar air collector systems with forced convection. Renewable Energy 83: 1119-1130. http://dx.doi.org/10.1016/j.renene.2015.03.009.

[4] Hüseyin B. (2013). Experimentally derived efficiency and exergy analysis of a new solar air heater having different surface shapes. Renewable Energy 50: 58-67. http://dx.doi.org/10.1016/j.renene.2012.06.022.

[5] S Bouadila, M Lazaar, S Skouri, S Kooli, A Farhat (2014). Energy and exergy analysis of a new solar air heater with latent storage energy. International Journal of Hydrogen Energy 39(27): 15266-15274. http://dx.doi.org/10.1016/j.ijhydene.2014.04.074.

[6] Chen GM, Alexander D, Paul K, Kostyantyn S. (2015). Comparative field experimental investigations of different flat plate solar collectors. Solar Energy 115: 577-588. http://dx.doi.org/10.1016/j.solener.2015.03.021.

[7] Hikmet E. (2008). Experimental energy and exergy analysis of a double-flow solar air heater having different obstacles on absorber plates. Building and Environment 43: 1046-1054. https://doi.org/10.1016/j.buildenv.2007.02.016.

[8] Farzaneh-Gord M, Arabkoohsar A, Deymi Dasht-bayaz M, Machado L, Koury RNN. (2014). Energy and exergy analysis of natural gas pressure reduction points equipped with solar heat and controllable heaters. Renewable Energy 72: 258-270. http://dx.doi.org/10.1016/j.renene.2014.07.019.

[9] Ahmad F, Kamaruzzaman S, Bakhtyar B, Mohamed G, Yusof OM, Hafidz RM. (2015). Review of solar drying systems with air based solar collectors in Malaysia. Renewable and Sustainable Energy Reviews 5: 1191-1204. http://dx.doi.org/10.1016/j.rser.2015.07.026.

[10] Golneshan AA, Nemati H. (2014). Exergy analysis of unglazed transpired solar collectors (UTCs). Solar Energy 107: 272-277. http://dx.doi.org/10.1016/j.solener.2014.04.025.

[11] Panwar NL, Kaushik SC, Surendran K. (2012). A review on energy and exergy analysis of solar dying systems. Renewable and Sustainable Energy Reviews 16: 2812-2819. https://doi.org/10.1016/j.rser.2012.02.053

[12] Park SR, Pandey AK, Tyagi VV, Tyagi SK. (2014). Energy and exergy analysis of typical renewable energy systems. Renewable and Sustainable Energy Reviews 30: 105-123. http://dx.doi.org/10.1016/j.rser.2013.09.011.

[13] Sabzpooshani M, Mohammadi K, Khorasanizadeh H. (2014). Exergetic performance evaluation of a single pass baffled solar air heater. Energy 64: 697-706. http://dx.doi.org/10.1016/j.energy.2013.11.046

[14] Kamal S, Ho HK, Su B. (2014). Sankey diagram framework for energy and exergy flows. Applied Energy 136, 1035-1042. http://dx.doi.org/10.1016/j.apenergy.2014.08.070.

[15] Ucar A, Inallı M. (2006). Thermal and exergy analysis of solar air collectors with passive augmentation techniques. International Communications in Heat and Mass Transfer 33, 1281-1290. https://doi.org/10.1016/j.icheatmasstransfer.2006.08.006

[16] Sanjay Y, Maneesh K, Varun S. (2014). Exergetic performance evaluation of solar air heater having arc shape oriented protrusions as roughness element. Solar Energy 105: 181-189. http://dx.doi.org/10.1016/j.solener.2014.04.001

[17] Singh KDP, Sharma SP. (2009). Analytical investigation on thermal performance of artificially roughened double flow solar air heater. ARISER 5: 1-7.

[18] Irfan K, Aydm D. (2004). Efficiency and exergy analysis of a new solar air heater. Renewable Energy 29: 1489-1501. https://doi.org/10.1016/j.renene.2004.01.006.

[19] Nwosu Nwachukwu P. (2010). Employing exergy-optimized pin fins in the design of an absorber in a solar air heater. Energy 35: 571-575. https://doi.org/10.1016/j.energy.2009.10.027.

[20] Kumar LM, Sarviya RM, Bhagoria JL. (2012). Exergy evaluation of packed bed solar air heater. Renewable and Sustainable Energy Reviews 16: 6262-6267. http://dx.doi.org/10.1016/j.rser.2012.04.024

[21] Farzad J, Emad A. (2013). Energetic and exergetic evaluation of flat plate solar collectors. Renewable Energy 56: 55-63. http://dx.doi.org/10.1016/j.renene.2012.10.031.

[22] Oztop Hakan F, Fatih B, Hepbasli A. (2013). Energetic and exergetic aspects of solar air heating (solar collector) systems. Renewable and Sustainable Energy Reviews 21: 59-83. http://dx.doi.org/10.1016/j.rser.2012.12.019.

[23] Bayraka Fatih, Oztop Hakan F, Hepbasli A. (2013). Energy and exergy analyses of porous baffles inserted solar air heaters for building applications. Energy and Buildings 57: 338-345. http://dx.doi.org/10.1016/j.enbuild.2012.10.055.

[24] Kalogirou Soteris A, Karellas Sotirios, Badescu Viorel, Braimakis Konstantinos. (2015). Exergy analysis on solar thermal systems: a better understanding of their sustainability. Renewable Energy: 1-6. http://dx.doi.org/10.1016/j.renene.2015.05.037.

[25] Mukesh Kumar S, Radha Krishna P. (2016). Exergy based performance evaluation of solar air heater with arc-shaped wire roughened absorber plate. Renewable Energy 96: 233-243. http://dx.doi.org/10.1016/j.renene.2016.04.083

[26] Sharma P, Saini JS, Varma HK (1991). Thermal performance of packed bed solar air heaters. Solar Energy 47: 59-67.

[27] Yeh HM, Ho CD, Hou JZ (2002). Collector efficiency of double-flow solar air heaters with fins attached. Energy 27: 715-727. S0360-5442(02)00010-5.

[28] Md Azharul K, Hawlader MNA (2006). Performance investigation of flat plate, v-corrugated and finned air collectors. Energy 31: 452-470. https://doi.org/10.1016/j.energy.2005.03.007.

[29] Abhishek P, Prabha C (2016). Thermal and thermohydraulic performance of wavy finned absorber solar air heater. Solar Energy 130: 250-259. http://dx.doi.org/10.1016/j.solener.2016.02.030.

[30] Kline SJ, McClintock FA (1953). Describing uncertainties in single sample experiments. Mech. Eng. 75: 3-8.

[31] Torres-Reyes E, Navarrete-Gonzalez JJ, Zaleta-Aguilar Z, Cervantesde Gortari JG (2003). Optimal process of solar to thermal energy conversion and design of irreversible flat-plate solar collectors. Energy 28: 99-113.